Electronic Supplementary Material (ESI) for ChemComm.

Electronic Supporting Information

Helical supramolecular polymerization of C_3-symmetric amides and retroamides: on the origin of cooperativity and handedness

Julia Buendía,[a] Joaquín Calbo,[b] Fátima García,[a] Juan Aragó,[b] Pedro M. Viruela,[b] Enrique Ortí,*[,b] and Luis Sánchez*[,a]

[a] *Departamento de Química Orgánica, Facultad de Ciencias Químicas, Universidad Complutense de Madrid, E-28040 Madrid (Spain). E-mail: lusamar@quim.ucm.es*

[b] *Instituto de Ciencia Molecular, Universidad de Valencia, 46980 Paterna (Spain). E-mail: enrique.orti@uv.es*

Contents:

1. Supplementary Figures

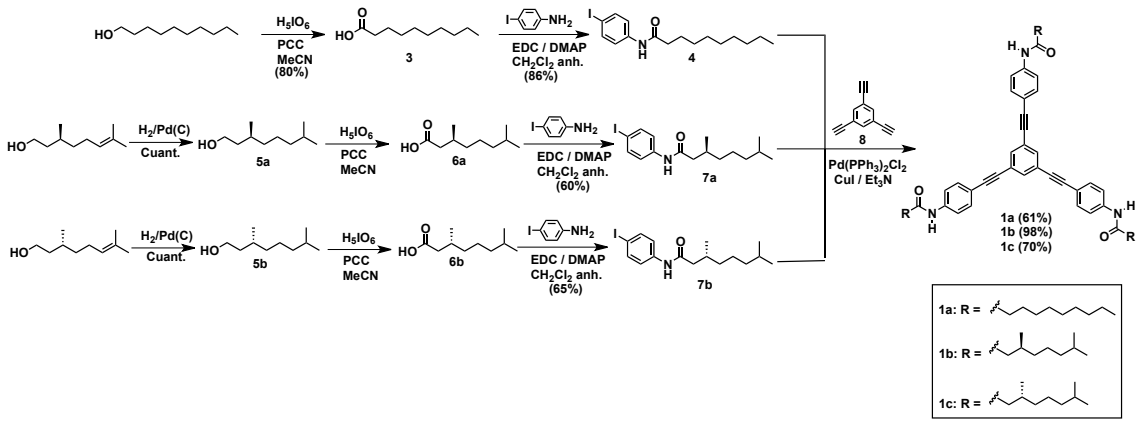

Scheme S1. Synthesis of N-centered trisamides **1a-c**.

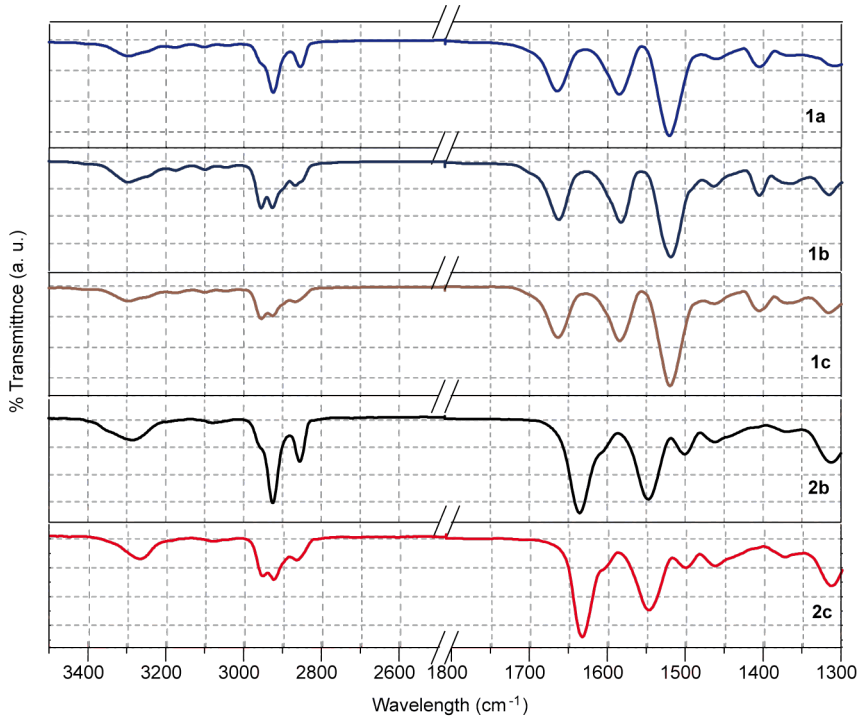

Figure S1. Partial FTIR spectra of trisamides **1a-c** and **2b-c**.

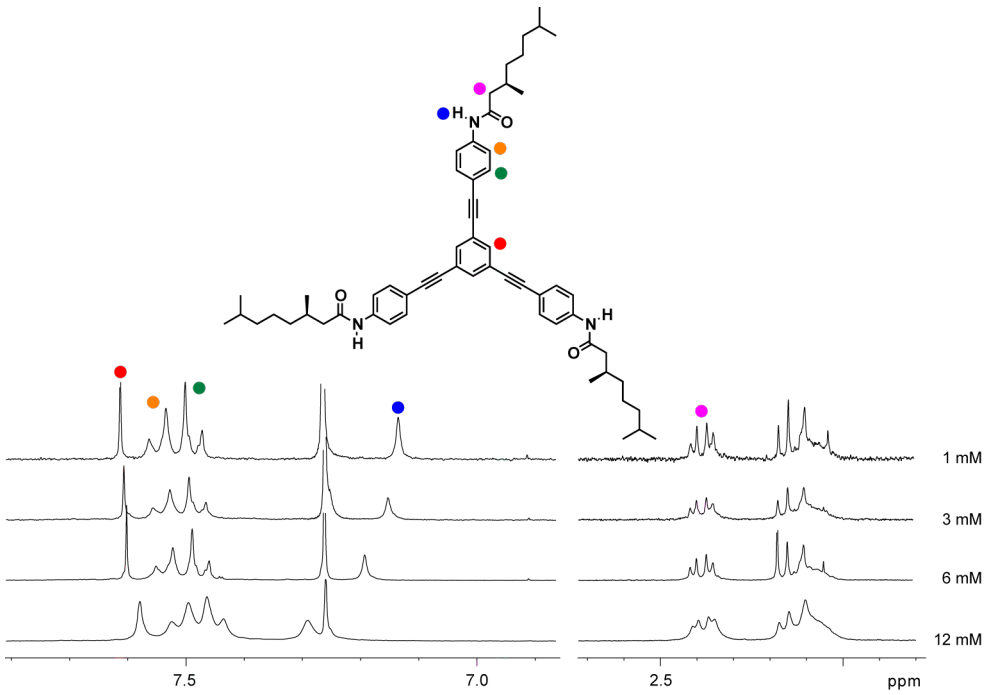

Figure S2. Partial concentration-dependent ^{1}H NMR spectra of **1c** in $CDCl_3$ (300 MHz, 298 K) showing the shift of the aromatic and amide protons.

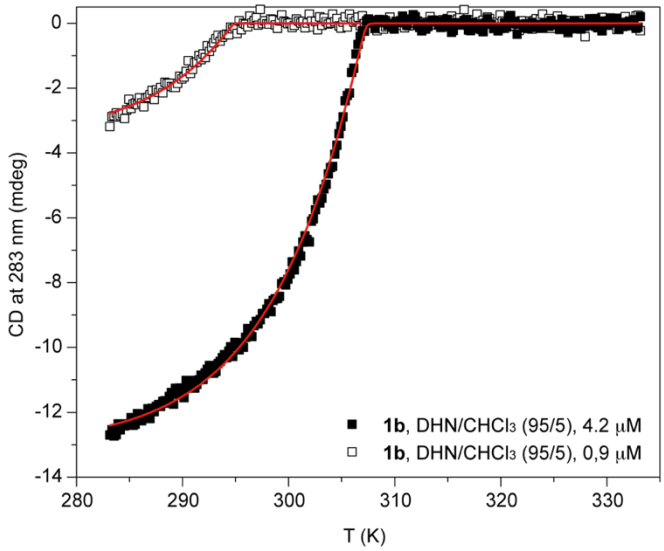

Figure S3. CD cooling curves of compound **1b** ($DHN/CHCl_3$, 95/5, measured at λ = 283 nm). Red lines correspond to the fitting to the EQ model.

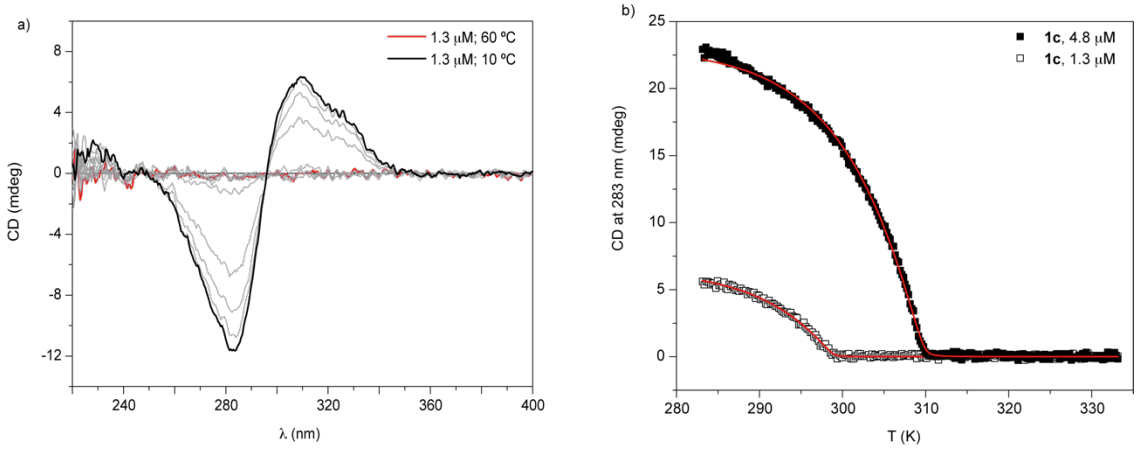

Figure S4. A) CD spectra of retroamide **1c** at temperatures ranging from 10 ºC (black line) to 60 ºC (red line). c) Cooling curves (1 K/min) of trisamide **1c** measured at λ = 283 nm. Red lines correspond to the fitting to the EQ model. All the experiments were performed in DHN/CHCl3 (95/5) solution.

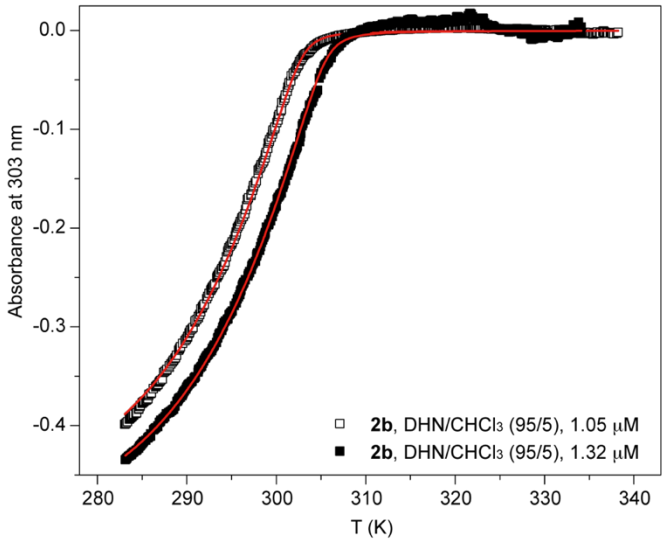

Figure S5. UV-Vis cooling curves of compound **2b** (DHN/$CHCl_3$, 95/5, measured at λ = 303 nm). Red lines correspond to the fitting to the EQ model.

2. Theoretical calculations

Theoretical Circular Dichroism

The theoretical circular dichroism (CD) electronic spectra for left- and right-handed trimers of **1** were computed at the B3LYP/6-31G* level of theory[1] using the time-dependent DFT (TD-DFT) approach.[2] The geometries used for the trimers correspond to those employed in the "Ideal Columnar Aggregates" section (see below), where the peripheral short $-C_5H_{11}$ chains bearing the stereogenic group (*R* or *S*) were substituted by methyl groups (Figure S6a) to alleviate the computational cost of the TD-DFT calculations. Calculations were performed for right-handed N-centered **1**-*P* and CO-centered **2**-*P* trimers and for the left-handed N-centered **1**-*M* trimer. The lowest-lying 100 singlet excited states were computed using the Tamm-Dancoff approximation (TDA).[3] The theoretical CD spectra (Figure 2b in the main text) were obtained after convolution of Gaussian functions (FWHM = 0.20 eV) centered at each electronic transition peak. All the calculations were performed by using the Gaussian 09 (revision D01) program package.[4]

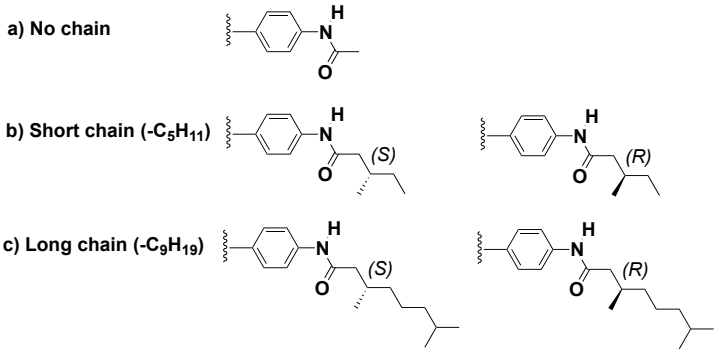

Figure S6. Chemical structure of the different peripheral alkyl chains utilized in the multi-level theoretical study of N-centered retroamines **1**. a) The alkyl chain is substituted by a methyl group. b) The alkyl chain is replaced by a short $-C_5H_{11}$ chain including the stereogenic center (*R* or *S*). c) Full alkyl chain including the stereogenic center (*R* or *S*).

---

[1] a) C. Lee, W. Yang, R. G. Parr, *Phys. Rev. B* **1988**, *37*, 785-789; b) A. D. Becke, *J. Chem. Phys.* **1993**, *98*, 5648-5652. c) M. M. Francl, W. J. Pietro, W. J. Hehre, J. S. Binkley, M. S. Gordon, D. J. Defrees, J. A. Pople, *J. Chem. Phys.* **1982**, *77*, 3654-3665.

[2] a) M. E. Casida, C. Jamorski, K. C. Casida, D. R. Salahub, *J. Chem. Phys.* **1998**, *108*, 4439-4449; b) C. Jamorski, M. E. Casida, D. R. Salahub, *J. Chem. Phys.* **1996**, *104*, 5134-5147; c) M. Petersilka, U. J. Gossmann, E. K. U. Gross, *Phys. Rev. Lett.* **1996**, *76*, 1212-1215.

[3] J. C. Taylor, *Physical Review* **1954**, *95*, 1313-1317.

[4] Gaussian 09, Revision D.01, M. J. Frisch, G. W. Trucks, H. B. Schlegel, G. E. Scuseria, M. A. Robb, J. R. Cheeseman, G. Scalmani, V. Barone, B. Mennucci, G. A. Petersson, H. Nakatsuji, M. Caricato, X. Li, H. P. Hratchian, A. F. Izmaylov, J. Bloino, G. Zheng, J. L. Sonnenberg, M. Hada, M. Ehara, K. Toyota, R. Fukuda, J. Hasegawa, M. Ishida, T. Nakajima, Y. Honda, O. Kitao, H. Nakai, T. Vreven, J. A. Montgomery, J. E. Peralta, F. Ogliaro, M. Bearpark, J. J. Heyd, E. Brothers, K. N. Kudin, V. N. Staroverov, R. Kobayashi, J. Normand, K. Raghavachari, A. Rendell, J. C. Burant, S. S. Iyengar, J. Tomasi, M. Cossi, N. Rega, J. M. Millam, M. Klene, J. E. Knox, J. B. Cross, V. Bakken, C. Adamo, J. Jaramillo, R. Gomperts, R. E. Stratmann, O. Yazyev, A. J. Austin, R. Cammi, C. Pomelli, J. W. Ochterski, R. L. Martin, K. Morokuma, V. G. Zakrzewski, G. A. Voth, P. Salvador, J. J. Dannenberg, S. Dapprich, A. D. Daniels, Farkas, J. B. Foresman, J. V. Ortiz, J. Cioslowski, D. J. Fox, Gaussian, Inc., Wallingford CT, 2009.

Molecular Mechanics/Molecular Dynamics Simulations

In order to shed light on the relative stability of the two possible columnar helices (i.e. clockwise *P* or anticlockwise *M*) in chirally substituted trisamides, a comprehensive molecular mechanics/molecular dynamics (MM/MD) study was performed for the aggregation of the N-centered retroamides **1** and the CO-centered carboxamides **2**. The TINKER 7.1 program package was used for all the MM/MD calculations.[5] A preliminary design of decamer models in right-handed (*P*) and left-handed (*M*) orientations was carried out for **1c** as a representative example (Figure S7), and the models were minimized by using the MM3 force field[6] without periodic conditions and a convergence criterion (RMS gradient per atom) of 0.01 kcal/mol/angstrom. Two different sizes of the peripheral alkyl chains bearing the stereogenic group (short chains of $–C_5H_{11}$ and long chains of $–C_9H_{19}$, Figure S6b and c, respectively) were used for the calculations in order to analyze the effect the length of the alkyl chain has on the relative stability of the two possible helices *P* and *M* (Figure S7). After full geometry relaxation of the π-stacked decamers with $–C_5H_{11}$ chains, both right-handed and left-handed helices of **1c** are computed practically at the same energy (–20.18 and –20.35 kcal/mol, respectively), though a slightly lower energy is predicted for the M-helix. Moving to the decamers with the $–C_9H_{19}$ chains, the energy difference between *P* and *M* is now of 3 kcal/mol (Figure S7) in favor of the *M*-helix, which suggests that the size of the alkyl chain is relevant for the energy differentiation between a right- and a left-handed growth of the columnar stacks. The intermolecular distance along the stacking axis (Δ*z*), computed as the average of the centroid-centroid distances between the core benzene rings of the three central molecules, is predicted to be very similar for all the decamers, ranging from 3.42 to 3.45 Å in the short-chain columns and being 3.45 Å in the long-chain decamers. The mean value for the rotational dihedral angle between adjacent monomers in the stack is predicted to be approximately 20º in the four oligomers (21.12 and –20.88º for the short-chain *P*- and *M*-helix, and 19.37 and –19.58º for the long-chain *P*- and *M*-helix, respectively). *P*- and *M*-decamers of **1b** and **2c** bearing long $–C_9H_{19}$ and $–C_{10}H_{21}$ chains, respectively, were also optimized using the MM3 approach and led to similar stacking distances (3.44–3.47 Å) and to an average twisting angle of 20º.

[5] J. W. Ponder, TINKER, Version 7.1; **2015**; http://dasher.wustl.edu/ tinker.
[6] N. L. Allinger, Y. H. Yuh, J. H. Lii, *J. Am. Chem. Soc* **1989**, *111*, 8551– 8566.

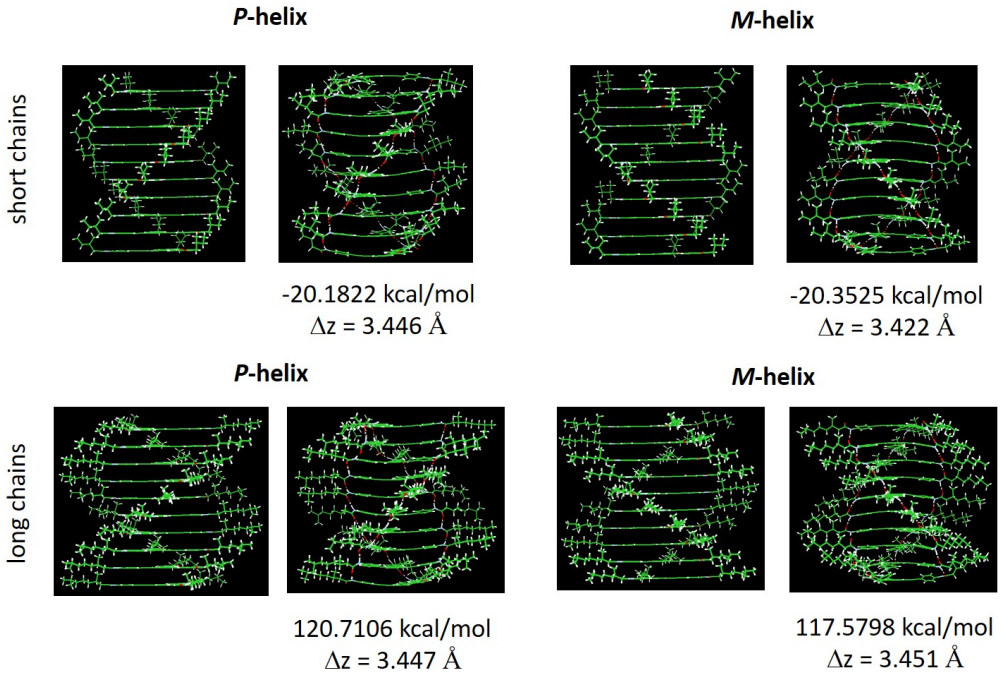

Figure S7. Initial geometry (left) and final MM3-optimized geometry (right) of right-handed (*P*) and left-handed (*M*) decamers of **1c**. Two different alkyl chains with the (*R*)-stereogenic center were modeled (Figure S6): short chains of $–C_5H_{11}$ (top) and long chains of $–C_9H_{19}$ (bottom). The final energy (in kcal/mol) and the average intermolecular distance (Δ*z* in Å) between adjacent monomeric units are given for the optimized geometries.

Taking into account the averaged intermolecular distance between monomers (Δ*z*) extracted from the decamer, and using a twisting angle of 20º between adjacent monomers along the stacking axis, unit cells containing 6 monomer units were modeled with translational periodic boundary conditions (see Figure S8). Since the system under study possesses C_3 symmetry, after 6 rotations of 20º, the repetition along the stacking direction (*z*-axis) is achieved.

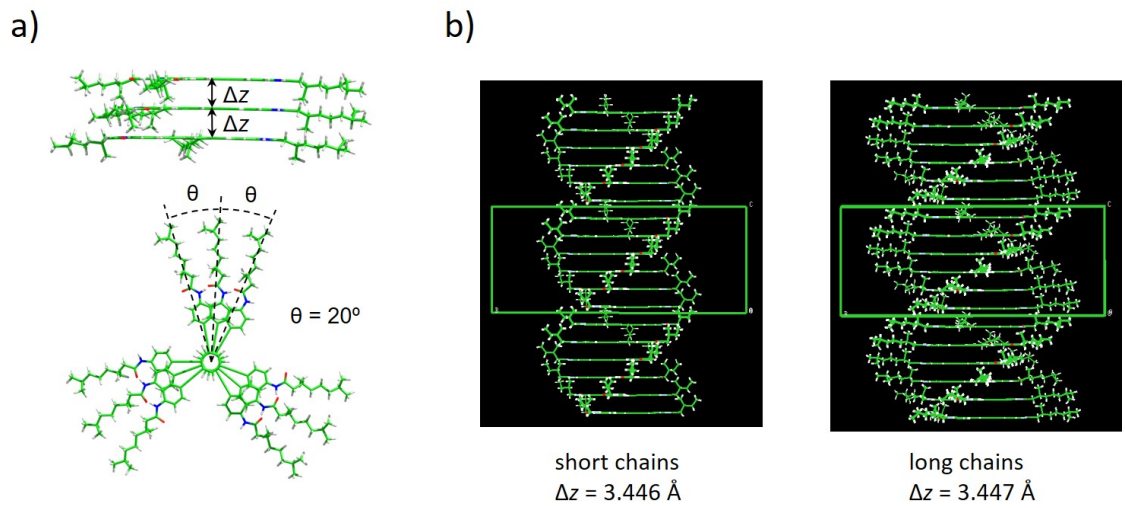

Figure S8. a) Stacking distance (Δ*z*) and twisting angle (*θ*) used to build-up the unit cell of a *P*-helix of **1c**. b) Periodic *P*-helices with short chains (left) and long chains (right) generated with unit cells containing 6 monomer units. The dimensions of the cell are (Δ*z* × 6, 50, 50) Å.

Long molecular dynamics on the modeled periodic aggregates with 100000 steps of 1.0 fs each (total dynamics time = 100 ps) were computed within the canonical (NVT) ensemble at 285 K for all the supramolecular stacks (*P*- and *M*-helices for short and long alkyl chains) of **1c**. The potential energy evolution along time for the different helices is shown in Figure S9. Similar MM/MD calculations were performed for compounds **1b** and **2c** with long alkyl chains and the evolution of the potential energy is shown in Figure S10. After the molecular dynamics, stabilizing binding energies per monomeric unit (E_{bind}) were calculated, by optimizing 200 snapshots along the MD trajectories corresponding to the last 50 ps of the production regime, according to the expression:

$$E_{\mathrm{bind}} = (E_{\mathrm{cell}} - nE_{\mathrm{mon}})/n, \qquad \text{(S1)}$$

where E_{cell} is the total energy of the unit cell, E_{mon} is the total energy of an isolated monomeric unit, and n is the number of molecules in the unit cell (n = 6).

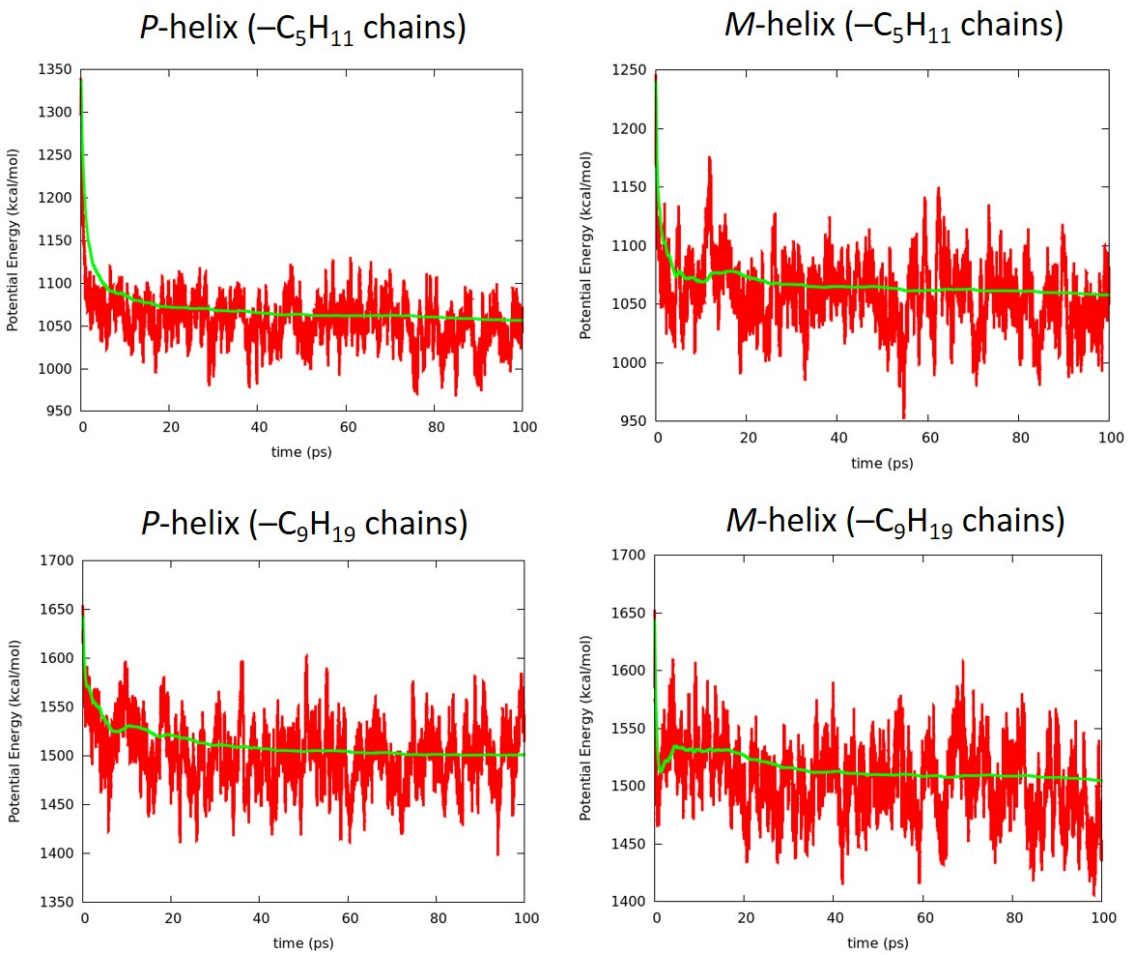

Figure S9. MM/MD potential energy as a function of time of the *P* (left) and *M* (right) helices of **1c** (*R* stereogenic center) bearing short (top) and long (bottom) alkyl chains. Absolute potential energies are shown in red and accumulated mean values are colored in green.

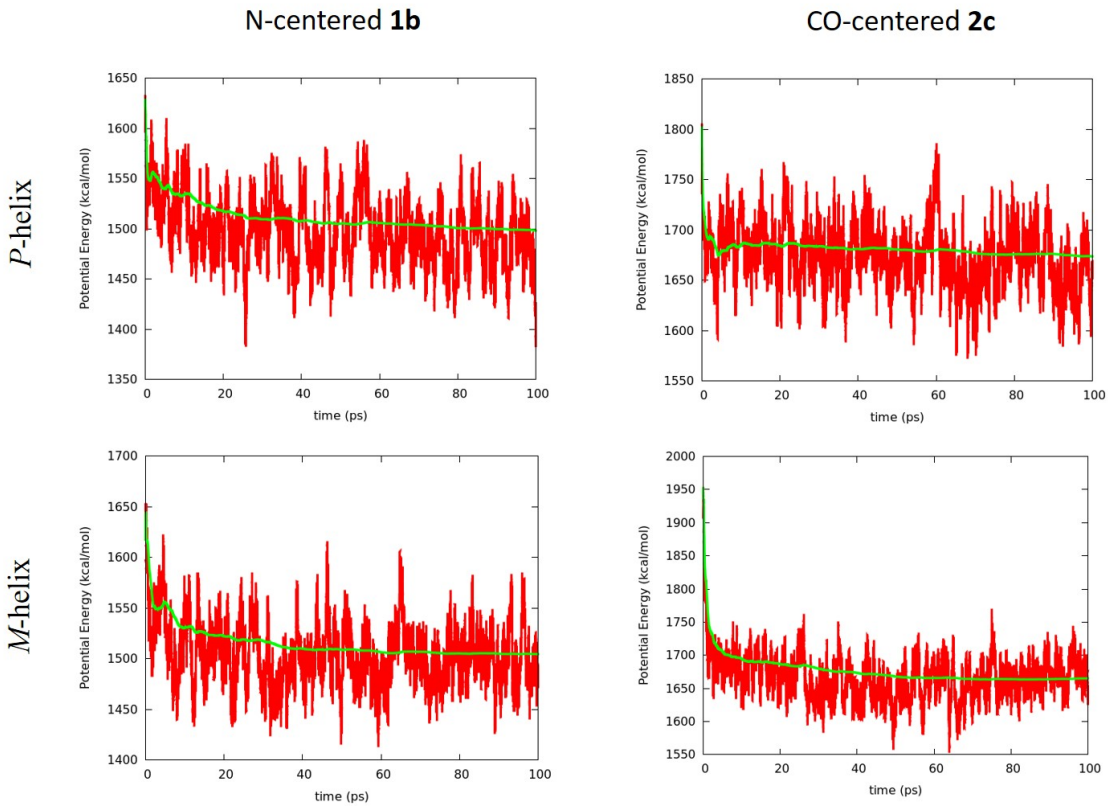

Figure S10. MM/MD potential energy as function of time of the supramolecular *P* (top) and *M* (bottom) helical aggregates formed by the N-centered retroamide **1b** (*S* stereogenic center) and the CO-centered carboxamide **2c** (*R* stereogenic center). Absolute potential energies are shown in red and accumulated mean values are colored in green.

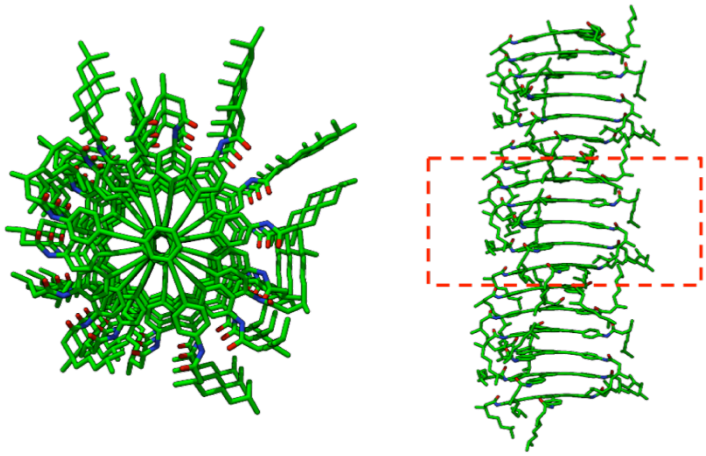

Figure S11. Top and side views of the most stable structure obtained from the MM/MD simulation for the left-handed *M*-helix of the *N*-centered retroamide **1c**. The unit cell containing six monomeric units is marked in dashed red lines. H atoms are omitted for clarity.

Ideal Columnar Aggregates

Columnar aggregates of increasing size of **1b** and **2b** were calculated at the DFT level using the hybrid meta exchange-correlation MPWB1K density functional,[7] and the 6-31G** basis set.[8] The MPWB1K functional was developed by Truhlar *et al.* to calculate thermochemical kinetics and noncovalent interactions. The attractiveness of the MPWB1K functional is that it successfully describes π-π stacking interactions and intermolecular hydrogen bonds using moderate basis sets.[9] Truhlar *et al.* reported a very comprehensive study on a large database of non-covalent interacting systems using different functionals and concluded that the MPWB1K functional gives good performance both for dispersion-dominated and for hydrogen-bonded interactions.[10] It has been successfully applied to describe stacked DNA base pairs,[11] to calculate the self-organization of bisurea macrocycles incorporating electroactive tetrathiafulvalene (TTF) units into supramolecular nanotubes through a combination of urea-urea hydrogen bonds and π-π stacking,[12] and to study the supramolecular helical polymerization of oligo(phenylene ethynylene) tricarboxamides.[13]

The geometry of **1b** and **2b** was first optimized for the isolated molecule using C_3 symmetry constraints with a symmetry axis passing through the center of the central benzene ring. The structure of the molecule was simplified by substituting the pendant alkyl $–C_9H_{19}$ and $–C_{10}H_{21}$ chains of the amide units in **1b** and **2b** by shorter $−C_5H_{11}$ and $−C_6H_{13}$ alkyl chains, respectively, bearing the stereogenic *S* center (Figure S12). Upon geometry relaxation, the central oligo(phenylene ethynylene) (OPE) moiety remains mostly planar both for **1b** and **2b**. However, there is an important difference in the conformation adopted by the amide groups. Whereas in **2b** they are twisted out of the molecular plane by 22.8º to minimize the steric interaction between the amide hydrogen and the vicinal benzene ring, in **1b** this interaction takes place at longer distances and the amide groups are mostly planar with the OPE core (Figure S12).

[7] Y. Zhao, D. G. Truhlar, *J. Phys. Chem. A* **2004**, *108*, 6908–6918.
[8] M. M. Francl, W. J. Pietro, W. J. Hehre, J. S. Binkley, M. S. Gordon, D. J. Defrees, J. A. Pople, *J. Chem. Phys.* **1982**, *77*, 3654–3665.
[9] (a) Y. Zhao, D. G. Truhlar, *J. Phys. Chem. A* **2005**, *109*, 5656−5667. (b) Y. Zhao, D. G. Truhlar, *J. Chem. Theory Comput.* **2005**, *1*, 415−432.
[10] Y. Zhao, D. G. Truhlar, *J. Chem. Theory Comput.* **2007**, *3*, 289–300.
[11] (a) Y. Zhao, D. G. Truhlar, *Phys. Chem. Chem. Phys.* **2005**, *7*, 2701–2705. (b) A. Dkhissi, R. Blossey, *J. Phys. Chem. B* **2008**, *112*, 9182–9186.
[12] J. L. López, E. M. Pérez, P. M. Viruela, R. Viruela, E. Ortí, N. Martín, *Org. Lett.* **2009**, *11*, 4524−4527.
[13] F. García, P. M. Viruela, E. Matesanz, E. Ortí, L. Sánchez, *Chem. Eur. J.* **2011***, 17*, 7755-7759.

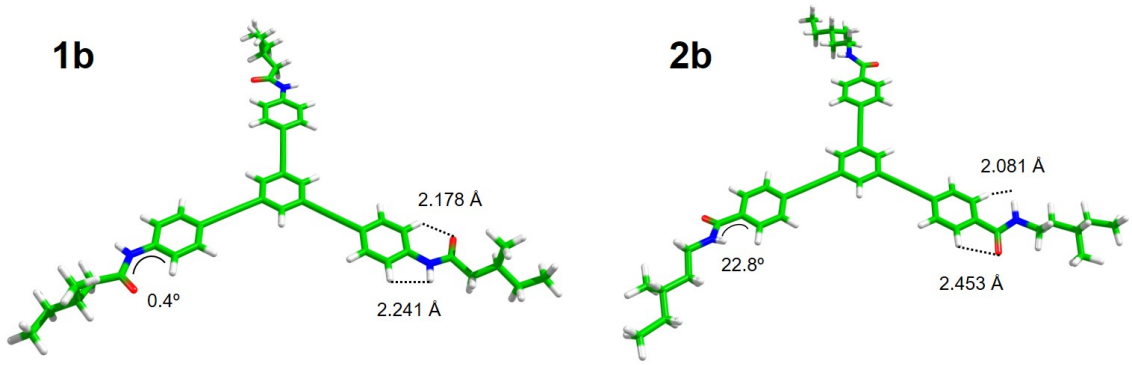

Figure S12. Minimum-energy structures calculated at the MPWB1K/6-31G** level for **1b** and **2b**. Selected interatomic distances (in Å) and torsional angles (in degrees) are indicated for the amide group. Carbon atoms are shown in green, hydrogen in white, nitrogen in blue, and oxygen in red.

The optimized monomer was used in a second step to generate C_3 pentamers for **1b** and **2b**. The molecules were initially stacked one over the other resembling the configuration obtained from the MD simulations (Figure S8), in which the π-conjugated backbone maximizes the π-interactions with the vicinal molecules and the units are slightly rotated around the perpendicular z-axis (approximately 20°) to allow the formation of efficient intermolecular hydrogen bonds between the amide groups. Keeping in mind that the preferred helical arrangement of **1b** and **2b** was shown to be a right-handed helix, the pentamers were built up in a *P*-helix conformation. The geometry of the pentamers was fully relaxed at the MPWB1K/6-31G** level and the optimized structures are shown in Figure S13a and S13b. Although the oligomer suffers from terminal effects and is deformed from the ideal infinite column, especially in the outer units, the model is large enough to consider that the central units provide adequate structural parameters to define the arrangement of the molecules along the columnar stack.

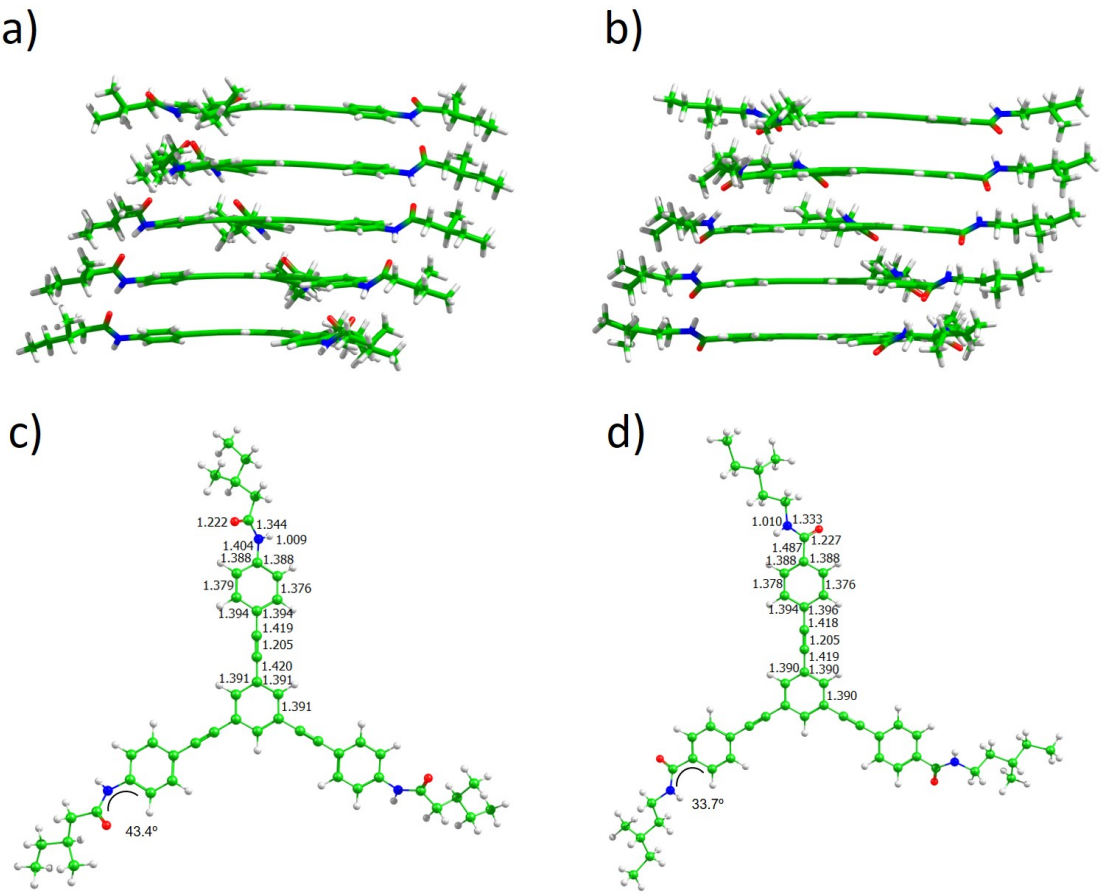

Figure S13. Minimum-energy MPWB1K/6-31G**-optimized C_3 structures calculated for the helical *P*-pentamer of **1b** (a) and **2b** (b). Optimized values for selected bond lengths (in Å) and torsional angles (in degrees) of the central molecule in the pentamer of **1b** (c) and **2b** (d).

The optimized geometry of the central molecule in the pentamer of **1b** and **2b** (Figure S13c and S13d, respectively) was used, in a third step, as the unit cell to generate face-to-face stacked C_3 aggregates of different length (n = 1−6, 8, 10 and 12). The averaged stacking parameters used to model the ideal columnar aggregates were an intermolecular distance Δz = 3.747 Å and an intermolecular rotation angle θ = 18.16º for $(\mathbf{1b})_n$, and Δz = 3.560 Å and θ = 18.00º for $(\mathbf{2b})_n$. Table S1 summarizes the values obtained for the stabilizing binding energy per monomer unit ($E_{\text{bind},n}$) calculated using the expression

$$E_{\text{bind},n} = (E_n - nE_{\text{mon}})/n,$$

where n is the number of monomers, E_n is the total energy of the $(\mathbf{1b})_n$ or $(\mathbf{2b})_n$ aggregate, and E_{mon} is the total energy calculated for the respective monomer using the geometry employed in the aggregate. The $(\mathbf{1b})_n$ aggregates were recalculated using the

correlation-consistent, triple-ζ quality cc-pVTZ basis set[14] and the MPWB1K/6-31G** geometries. The cc-pVTZ basis implies a huge increase in the number of basis functions involved in the calculation of the (**1b**)$_n$ aggregates. For the largest aggregate (n = 12, 1260 atoms), the number of basis functions increases from 12780 (6-31G**) to 28008 (cc-pVTZ). The employment of the more extended cc-pVTZ basis set determine a decrease of the basis set superposition error (BSSE), always present in a supramolecular calculation of interacting molecular fragments, and leads to a reduction of ~20% in the values obtained for the stabilization energy per monomer unit (Table S1).

Table S1. Stabilizing binding energies per monomer unit ($E_{bind,n}$, in kJ/mol) calculated for (**1b**)$_n$ and (**2b**)$_n$ aggregates as a function of the number of monomers (n) using the MPWB1K functional. The basis set employed in the calculation is indicated within parentheses.

n	**1b** (6-31G**)	**1b** (cc-pVTZ)	**2b** (6-31G**)
1	0.000	0.000	0.000
2	–58.171	–44.602	–42.294
3	–83.307	–64.046	–63.703
4	–93.380	–75.736	–75.417
5	–106.076	–82.442	–82.895
6	–111.808	–87.371	–88.043
8	–119.489	–94.178	–94.556
10	–123.698	–97.555	–98.388
12	–127.333	–100.728	–100.973

Figure 3c in the main text and Figure S14 display the evolution of $E_{bind,n}$ computed at the MPWB1K/6-31G** and MPWB1K/cc-pVTZ level, respectively, for ideal (**1b**)$_n$ aggregates as the number of monomer units increases. The $E_{bind,n}$ values were fitted to the following biexponential function:

$$y = A_1 e^{-x/b_1} + A_2 e^{-x/b_2} + y_0,$$

where x denotes the number of monomers (n). The asymptotic binding energy calculated for $n = \infty$ is –129.87 kJ/mol when using the 6-31G** basis set, and reduces to –104.35 kJ/mol when the more extended cc-pVTZ basis set is employed. Figure

[14] T. H. Dunning, Jr., *J. Chem. Phys.* **1989**, *90*, 1007–1023; D. Woon, T. H. Dunning, Jr., *J. Chem. Phys.* **1995**, *103*, 4572–4585.

S15a shows the evolution The $E_{bind,n}$ values computed at the MPWB1K/6-31G** level for $(\mathbf{2b})_n$ aggregates led to an asymptotic binding energy of –105.33 kJ/mol for $n = \infty$.

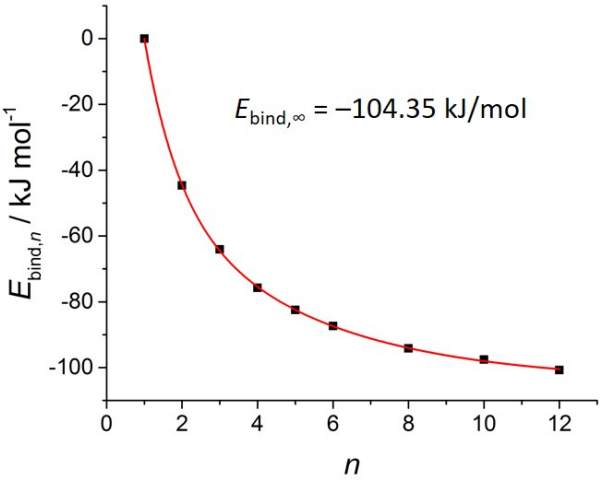

Figure S14. Binding energy per monomer unit ($E_{bind,n}$) as the number of monomers (n) in the $(\mathbf{1b})_n$ aggregate increases calculated at the MPWB1K/cc-pVTZ level, and fit (red line) to a biexponential decay.

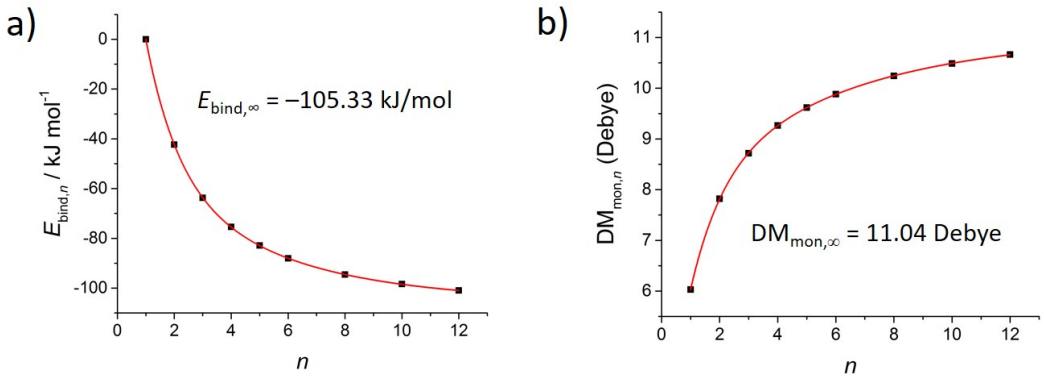

Figure S15. a) Binding energy per monomer unit ($E_{bind,n}$) as the number of monomers (n) in the $(\mathbf{2b})_n$ aggregate increases calculated at the MPWB1K/6-31G** level, and fit (red line) to a biexponential decay. b) Dipole moment per monomer unit ($DM_{mon,n}$) calculated for $(\mathbf{2b})_n$ at the at the MPWB1K/6-31G** level, and fit to a biexponential function.

In order to analyze the evolution of the dipole moment with the size of the columnar aggregate, theoretical dipole moments were computed at the MPWB1K/6-31G** level. Figure 3d in the main text and Figure S15b show the evolution, as the number of monomer units increases, of the dipole moment per monomer unit ($DM_{mon,n}$) calculated

for the (**1b**)$_n$ and (**2b**)$_n$ aggregates, respectively. The $DM_{mon,n}$ values were fitted to the following biexponential function:

$$y = A_1 e^{-x/b_1} + A_2 e^{-x/b_2} + y_0,$$

where *x* denotes the number of monomers (*n*). The increase of $DM_{mon,n}$ with *n* is due to the enhancement of the polarization of the H-bonding network as the aggregate increases, and is a clear indication of the cooperative character of the supramolecular polymerization process. The asymptotic value predicted for $DM_{mon,\infty}$ is 12.94 D for (**1b**)$_n$ and 11.04 D for (**2b**)$_n$. The higher value obtained for the N-centered retroamide **1** in comparison with the CO-centered carboxamide **2** suggests a higher degree of cooperativity for the former.

3. Experimental section

General. All solvents were dried according to standard procedures. Reagents were used as purchased. All air-sensitive reactions were carried out under argon atmosphere. Flash chromatography was performed using silica gel (Merck, Kieselgel 60, 230-240 mesh or Scharlau 60, 230-240 mesh). Analytical thin layer chromatography (TLC) was performed using aluminium-coated Merck Kieselgel 60 F254 plates. NMR spectra were recorded on a Bruker Avance 300 (^{1}H: 300 MHz; ^{13}C: 75 MHz) spectrometer at 298 K using partially deuterated solvents as internal standards. Coupling constants (*J*) are denoted in Hz and chemical shifts (δ) in ppm. Multiplicities are denoted as follows: s = singlet, d = doublet, t = triplet, m = multiplet, br = broad. FT-IR spectra were recorded on a Bruker Tensor 27 (ATR device) spectrometer. UV-Vis spectra were registered on a Jasco-V630 spectrophotometer equipped with a Peltier thermoelectric temperature controller. A 1 mm path length quartz cuvette (Hellma) was used. Circular dichroism (CD) measurements were performed on a Jasco-810 dichrograph equipped with a Peltier thermoelectric temperature controller. The spectra were recorded in the continuous mode between 400 and 200 nm, with a wavelength increment of 1 nm, a response time of 4 s, and a bandwidth of 1 nm. A 1 cm path length quartz cuvette (Hellma) was used. High resolution mass spectra (HRMS) were recorded on a FTMS Bruker APEX Q IV spectrometer.

4. Synthetic details and characterization

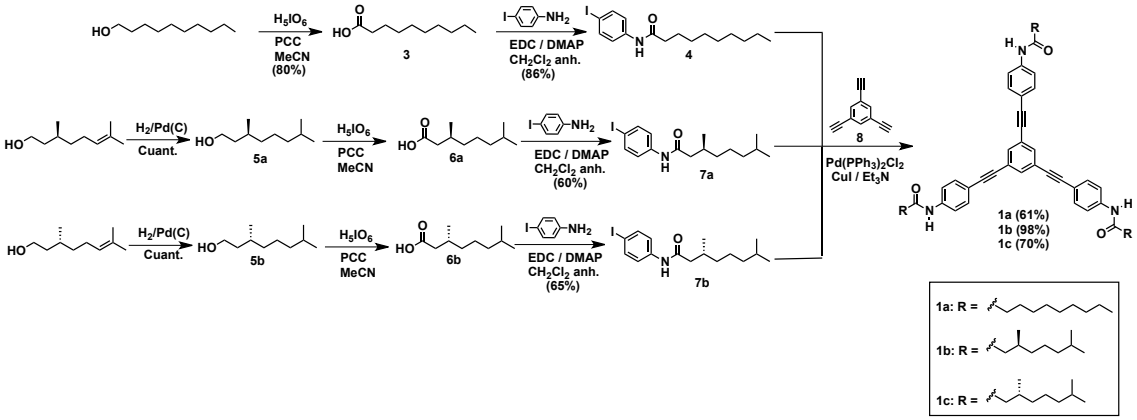

Compounds **3**[15] **4**,[16] **6a**,[17] and **6b**[17] were prepared according to previously reported synthetic procedures and showed identical spectroscopic properties to those reported therein.

(*S*)-N-(4-iodophenyl)-3,7-dimethyloctanamide (7a)

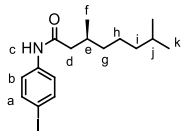

Chemical Formula: $C_{16}H_{24}INO$
Exact Mass: 373.0903
Molecular Weight: 373.2723

Compound **6a** (1.04 g, 6.04 mmol), 1-ethyl-3-(3-dimethylaminopropyl)carbo-diimide hydrochloride (1.27 g, 6.64 mmol) and 4-dimethylaminopyridine (0.81 g, 6.64 mmol) were dissolved in dry methylene chloride (20 mL) under argon atmosphere. The mixture was cooled to 0 ºC and stirred for 15 minutes. Then, 4-iodoaniline (1.32 g, 6.04 mmol) was added portionwise. The reaction mixture was stirred at room temperature overnight. The organic layer was washed with HCl 1 M, NaOH 3M and water and dried over $MgSO_4$. The solvent was evaporated under reduced pressure affording **7a** as a white solid (1.41 g, 60%).^{1}H NMR ($CDCl_3$, 300 MHz) δ 7.60 (2H, H_a, d, J = 8.7); 7.31 (3H, H_{b+c}, d, J = 8.7); 2.36 (1H, H_e, m); 2.10 (2H, H_d, m); 1.55 (1H, H_j, m); 1.35–1.10 (6H, H_{g+h+i}, br); 0.97 (3H, H_f, d, J = *6.4*); 0.86 (6H, H_k, d, J = *6.4*). ^{13}C NMR ($CDCl_3$, 75 MHz) δ 171.12, 137.91, 137.72, 121.70, 87.32, 45.65, 39.08, 37.46, 31.27, 27.97, 25.12, 23.07, 22.95, 20.11. FTIR (neat) 696, 817, 938, 974, 1007, 1295, 1387, 1462, 1478, 1520, 1587, 1632, 1660, 2862, 2927, 2954, 3301 cm^{-1}.

[15] M. Szostak, M. Spain and D. J. Procter, *J. Am. Chem. Soc.,* 2014, ***136***, 8459.
[16] A. Mori, I. Akahoshi, M. Hashimoto, T, Doi and T. Takahashi*, Liquid Crystals* 2010, **3,** 1361.
[17] M. M. L. Nieuwenhuizen, T. F. A. De Greef, R. L. J. Van der Bruggen, J. M. J. Paulusse, W. P. J. Appel, M. M. J. Smulders, R. P. Sijbesma and E. W. Meijer, *Chem. Eur. J.* 2010, **16**, 1601.

(*R*)-N-(4-iodophenyl)-3,7-dimethyloctanamide (7b)

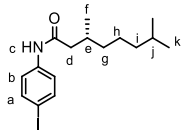

Chemical Formula: $C_{16}H_{24}INO$
Exact Mass: 373.0903
Molecular Weight: 373.2723

Compound **6b** (0.21 g, 1.22 mmol), 1-ethyl-3-(3-dimethylaminopropyl)carbo-diimide hydrochloride (0.26 g, 1.34 mmol) and 4-dimethylaminopyridine (0.16 g, 1.34 mmol) were dissolved in dry methylene chloride (10 mL) under argon atmosphere. The mixture was cooled to 0 ºC and stirred for 15 minutes. Then, 4-iodoaniline (0.27 g, 1.22 mmol) was added portionwise. The reaction mixture was stirred at room temperature overnight. The organic layer was washed with HCl 1 M, NaOH 3M and water and dried over $MgSO_4$. The solvent was evaporated under reduced pressure affording **7b** as a white solid (0.29 g, 65%).^{1}H NMR ($CDCl_3$, 300 MHz) δ 7.60 (2H, H_a, d, J = 8.7); 7.30 (2H, H_b, d, J = 8.7); 7.17 (1H, H_c, br); 2.35 (1H, H_e, m); 2.09 (2H, H_d, m); 1.52 (1H, H_j, m); 1.40–1.08 (6H, H_{g+h+i}, br); 0.97 (3H, H_f, d, J = 6.4); 0.86 (6H, H_k, d, J = 6.4). ^{13}C NMR ($CDCl_3$, 75 MHz) δ 171.39, 138.29, 138.07, 122.01, 87.67, 46.04, 39.44, 37.46, 31.27, 28.34, 25.12, 23.07, 22.95, 20.11. FTIR (neat) 694, 817, 938, 974, 1007, 1295, 1387, 1462, 1478, 1520, 1587, 1632, 1660, 2860, 2928, 3300 cm^{-1}.

Compound 1a

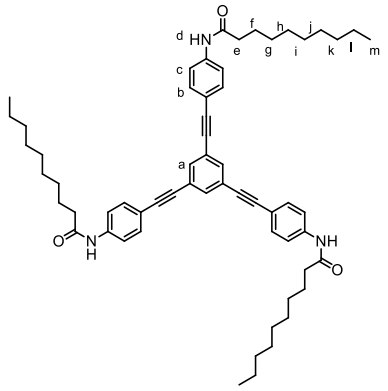

Chemical Formula: $C_{60}H_{75}N_3O_3$
Exact Mass: 885.58
Molecular Weight: 886.26

Compound **4** (0.92 g, 2.38 mmol), compound **8** (0.11 g, 0.72 mmol), bis-(triphenylphosphine)-palladium(II) chloride (0.03 g, 0.036 mmol), copper(I) iodide (0.008 g, 0.043 mmol), were dissolved in dry THF (20 mL) and subjected to several vacuum/argon cycles. After that, triethylamine (4 mL) was added and subjected to more vacuum/argon cycles. The reaction mixture was heated at 67 ºC and stirred 22 hours. After evaporation of the solvent under reduced pressure, the residue was washed with HCl 1M, extracted with chloroform, washed again with NH_4Cl saturated

solution and water and dried over $MgSO_4$. After evaporation of the solvent, the residue was purified by column chromatography (silica gel, chloroform) affording compound **1a** as a yellow solid (0.39 g, 61%). ^{1}H NMR ($CDCl_3$, 500 MHz) δ 7.60 (3H, H_a, s); 7.53 (6H, H_c, d, J = 8.2); 7.47 (6H, H_b, d, J = 8.2); 7.20 (3H, H_d, s); 2.37 (6H, H_e, t, J = 7.5), 1.73 (6H, H_f, m), 1.40–1.27 (36H, $H_{g+h+i+j+k+l}$, br); 0.88 (9H, H_m, t, J = 6.7. ^{13}C NMR ($CDCl_3$, 125 MHz) δ 171.30, 138.32, 133.77, 132.52, 131.72, 124.18, 119.51, 118.46, 90.30, 87.60, 65.92, 37.85, 31.83, 29.40, 29.34, 29.26, 29.22, 25.53, 22.61, 15.37, 13.98. FTIR (neat) 877, 1177, 1248, 1405, 1460, 1521, 1585, 1665, 2855, 2924, 3297 cm^{-1}. HRMS (MALDI-TOF): calc. for $C_{60}H_{76}N_3O_3$ $[M+H]^+$ 886.5886; found 886.5836.

Compound 1b

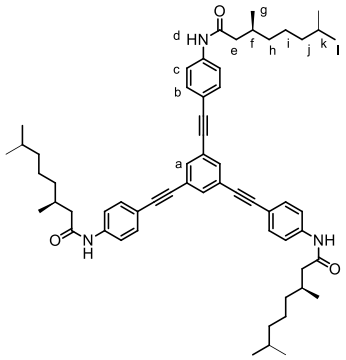

Compound **7a** (1.04 g, 2.68 mmol), compound **8** (0.12 g, 0.81 mmol), bis-(triphenylphosphine)-palladium(II) chloride (0.028 g, 0.04 mmol), copper(I) iodide (0.009 g, 0.048 mmol), were dissolved in dry THF (10 mL) and subjected to several vacuum/argon cycles. After that, triethylamine (2.5 mL) was added and subjected to more vacuum/argon cycles. The reaction mixture was heated at 67 ºC and stirred 25 hours. After evaporation of the solvent under reduced pressure, the residue was washed with HCl 1M, extracted with chloroform, washed again with NH_4Cl saturated solution and water and dried over $MgSO_4$. After evaporation of the solvent, the residue was purified by column chromatography (silica gel, chloroform) affording compound **1b** as a yellow solid (2.3 g, 98%). ^{1}H NMR ($CDCl_3$, 500 MHz) δ 7.58 (6H, H_d, s); 7.50 (3H, H_a, s); 7.43 (6H, H_c, d, J = 8.3); 7.37 (6H, H_b, d, J = 8.3); 2.38 (3H, H_e, m); 2.15 (3H, H_e, m); 2.07 (3H, H_f, m); 1.53 (3H, H_k, m); 1.41–1.12 (18H, H_{h+i+j}, m), 0.99 (9H, H_g, d, J = 6.6), 0.87 (18H, H_l, d, J = 6.6). ^{13}C NMR ($CDCl_3$, 125 MHz) δ 171.69, 138.41, 134.06, 132.82, 124.35, 120.30, 118.95, 90.59, 88.06, 45.93, 39.50, 37.53, 31.31, 28.36, 25.17, 23.09, 22.97, 20.13. FTIR (neat) 835, 875, 1028, 1116, 1246, 1316, 1405, 1463, 1519, 1584, 1663, 2867, 2955, 3297 cm^{-1}. HRMS (MALDI-TOF): calc. for $C_{60}H_{76}N_3O_3$ $[M+H]^+$ 886.5886; found 886.5892.

Compound 1c

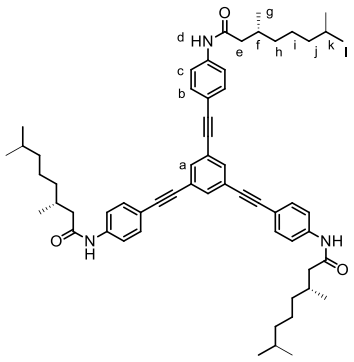

Chemical Formula: $C_{60}H_{75}N_3O_3$
Exact Mass: 885.5808
Molecular Weight: 886.2558

Compound **7b** (1.0 g, 2.58 mmol), compound **8** (0.12 g, 0.78 mmol), bis-(triphenylphosphine)-palladium(II) chloride (0.027 g, 0.039 mmol), copper(I) iodide (0.009 g, 0.047 mmol), were dissolved in dry THF (20 mL) and subjected to several vacuum/argon cycles. After that, triethylamine (4 mL) was added and subjected to more vacuum/argon cycles. The reaction mixture was heated at 67 ºC and stirred 24 hours. After evaporation of the solvent under reduced pressure, the residue was washed with HCl 1M, extracted with chloroform, washed again with NH_4Cl saturated solution and water and dried over $MgSO_4$. After evaporation of the solvent, the residue was purified by column chromatography (silica gel, chloroform) affording compound **1c** as a yellow solid (1.5 g, 60%). ^{1}H NMR ($CDCl_3$, 500 MHz) δ 7.57 (3H, H_a, s); 7.50 (6H, H_c, d, J = 8.1); 7.45 (6H, H_b, d, J = 8.1); 7.26 (3H, H_d, s); 2.38 (3H, H_e, m); 2.14 (3H, H_e, m); 2.07 (3H, H_f, m); 1.53 (3H, H_k, m); 1.40–1.13 (18H, H_{h+i+j}, m), 0.99 (9H, H_g, d, J = 6.4), 0.87 (18H, H_l, d, J = 6.4). ^{13}C NMR ($CDCl_3$, 125 MHz) δ 171.17, 138.20, 133.89, 132.64, 124.18, 119.69, 118.54, 90.38, 87.73, 45.81, 39.22, 37.25, 31.05, 28.10, 24.89, 22.83, 22.71, 19.88. FTIR (neat) 835, 876, 1113, 1247, 1315, 1405, 1463, 1518, 1583, 1662, 2867, 2926, 2955, 3297 cm^{-1}. HRMS (ESI-FT): calc. for $C_{60}H_{74}N_3O_3$ $[M\text{-}H]^+$, 884.57357 found, 884.57619.

5. Collection of spectra

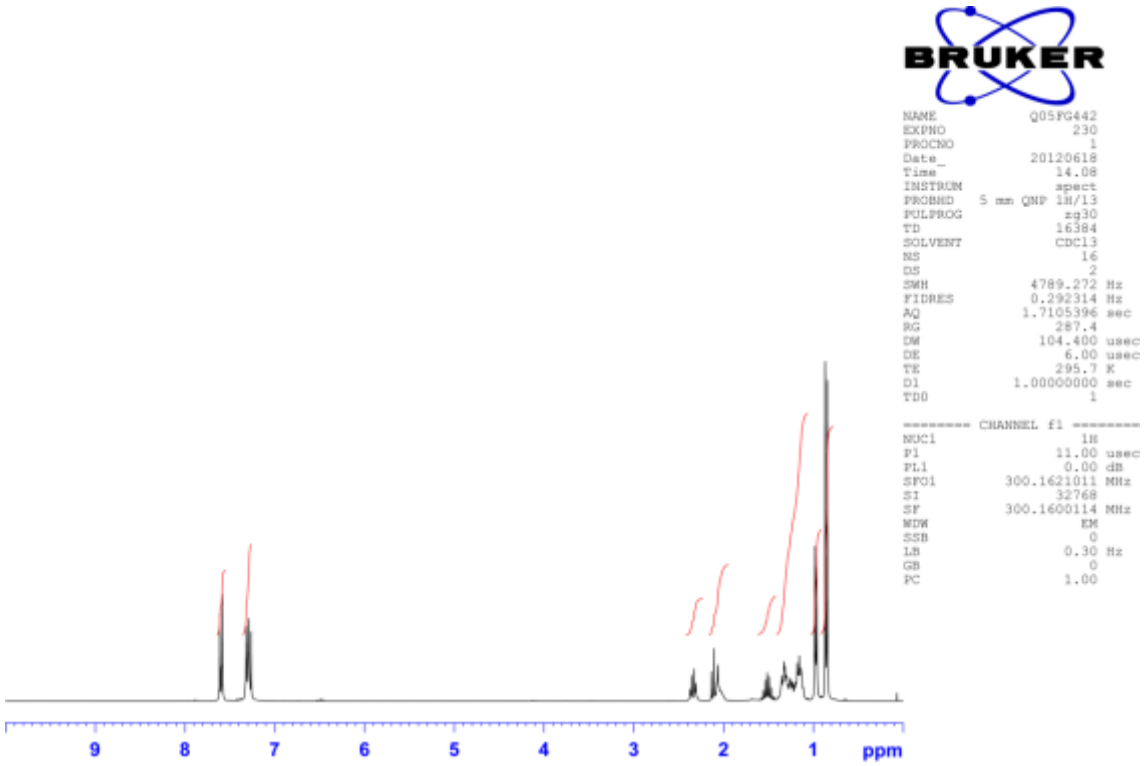

^{1}H NMR ($CDCl_3$, 300 MHz, 298 K) of compound **7a.**

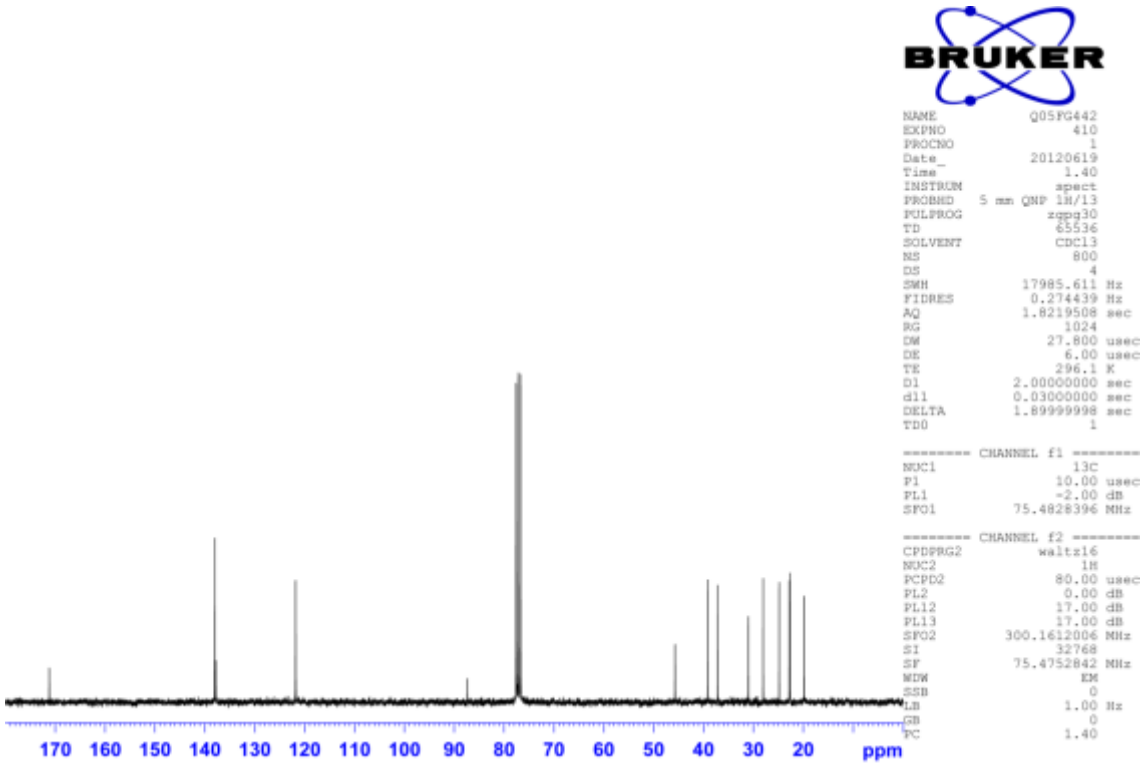

^{13}C NMR ($CDCl_3$, 75 MHz, 298 K) of compound **7a**.

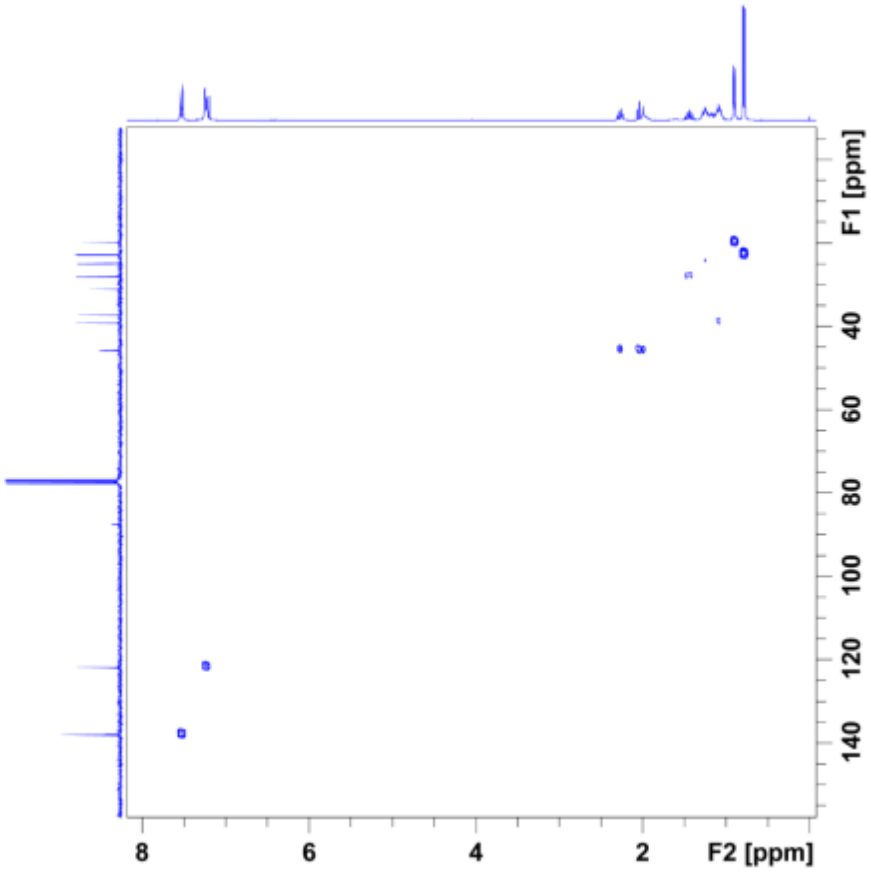

^{1}H, ^{13}C-HMQC spectrum ($CDCl_3$, 298 K) of compound **7a**.

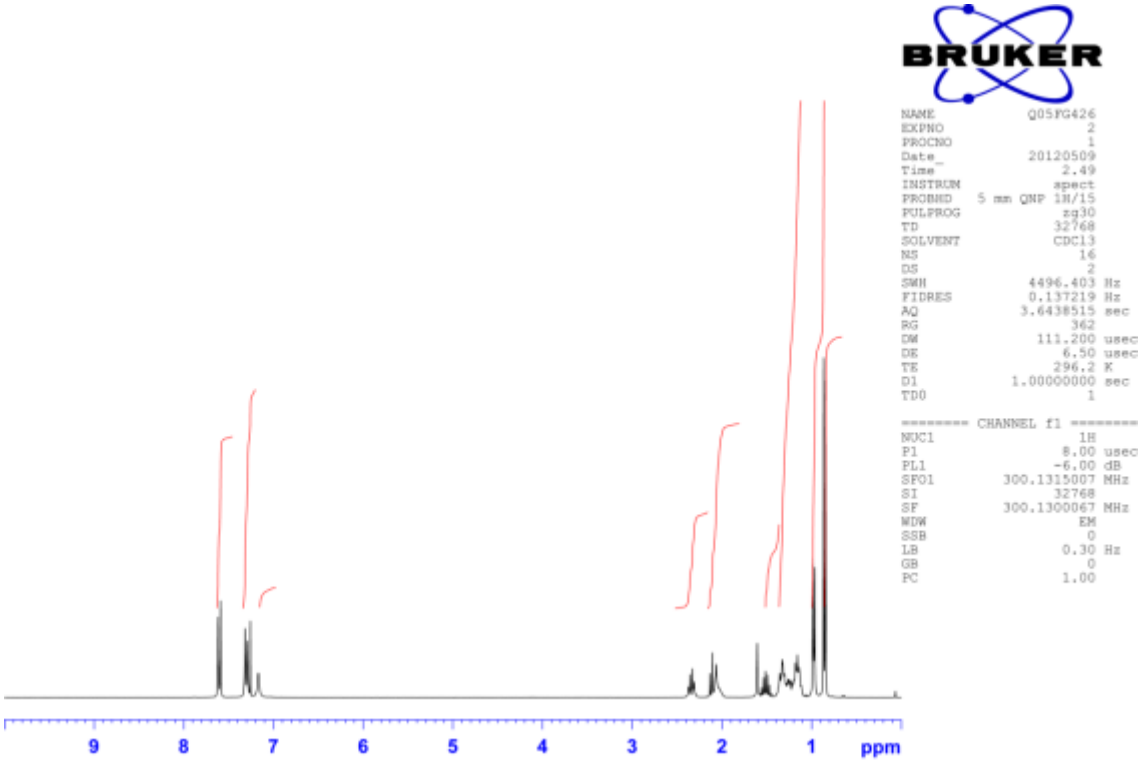

^{1}H NMR ($CDCl_3$, 300 MHz, 298 K) of compound **7b**.

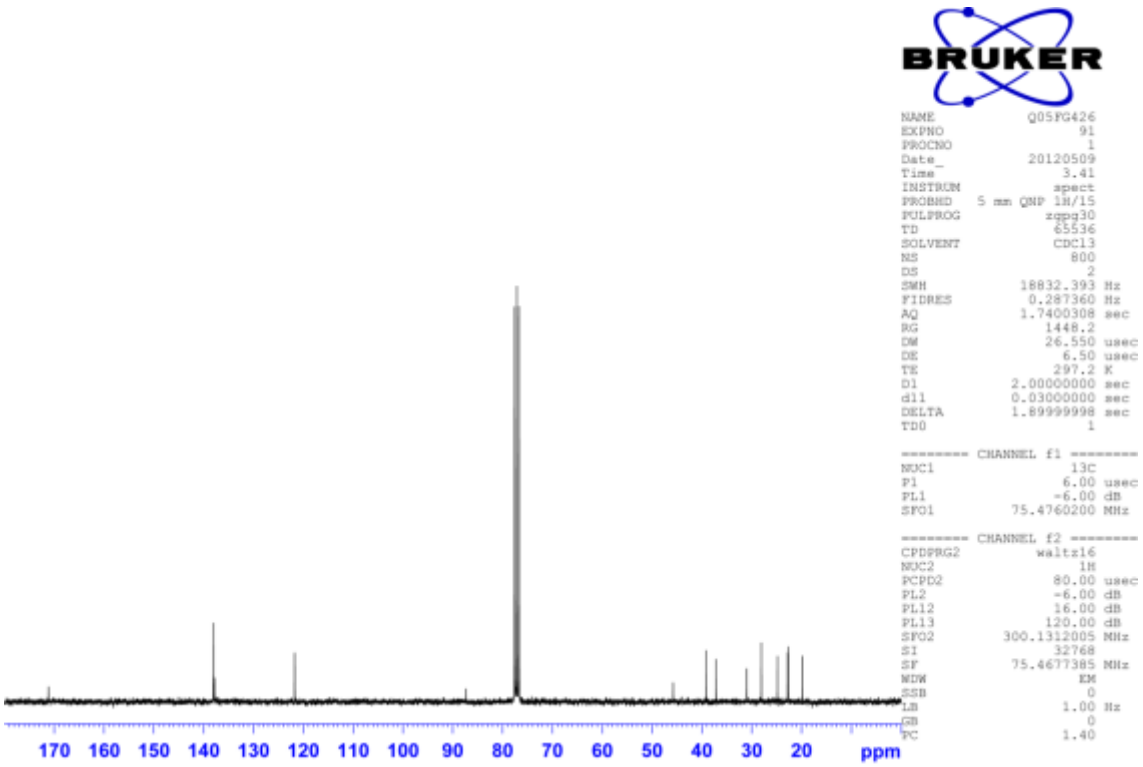

^{13}C NMR ($CDCl_3$, 75 MHz, 298 K) of compound **7b**.

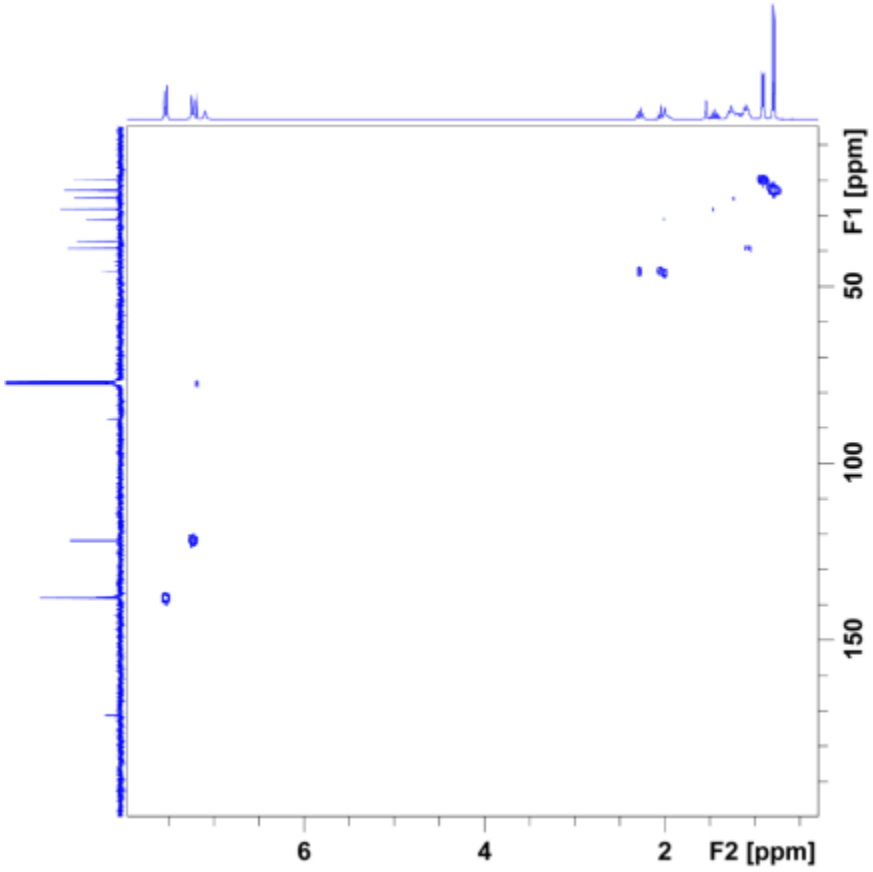

^{1}H, ^{13}C-HMQC spectrum ($CDCl_3$, 298 K) of compound **7b**.

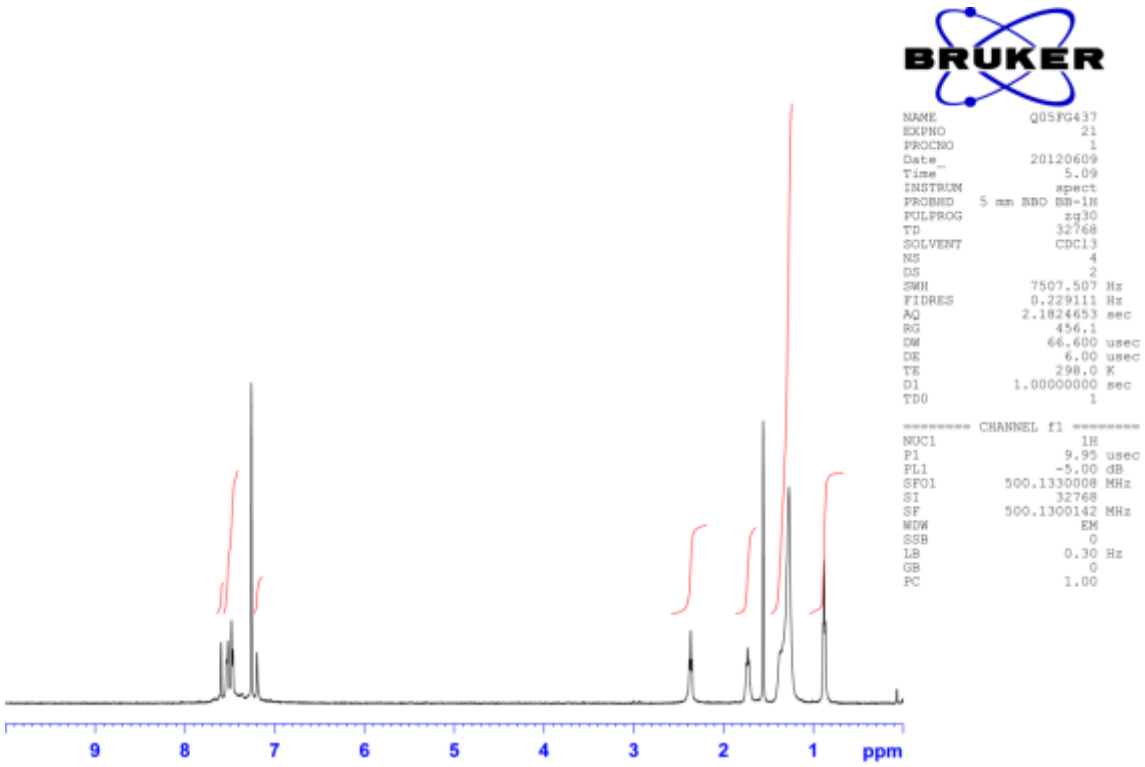

^{1}H NMR ($CDCl_3$, 500 MHz, 298 K) of compound **1a**.

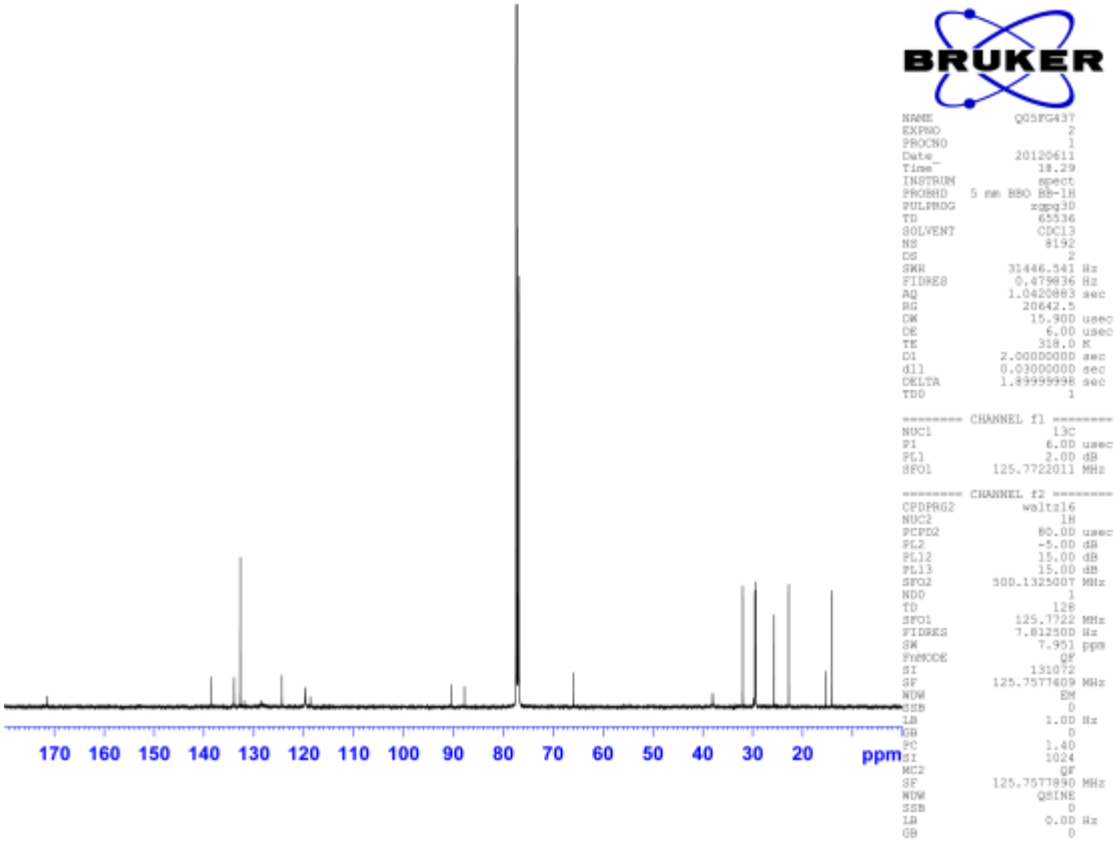

^{13}C NMR ($CDCl_3$, 125 MHz, 318 K) of compound **1a**.

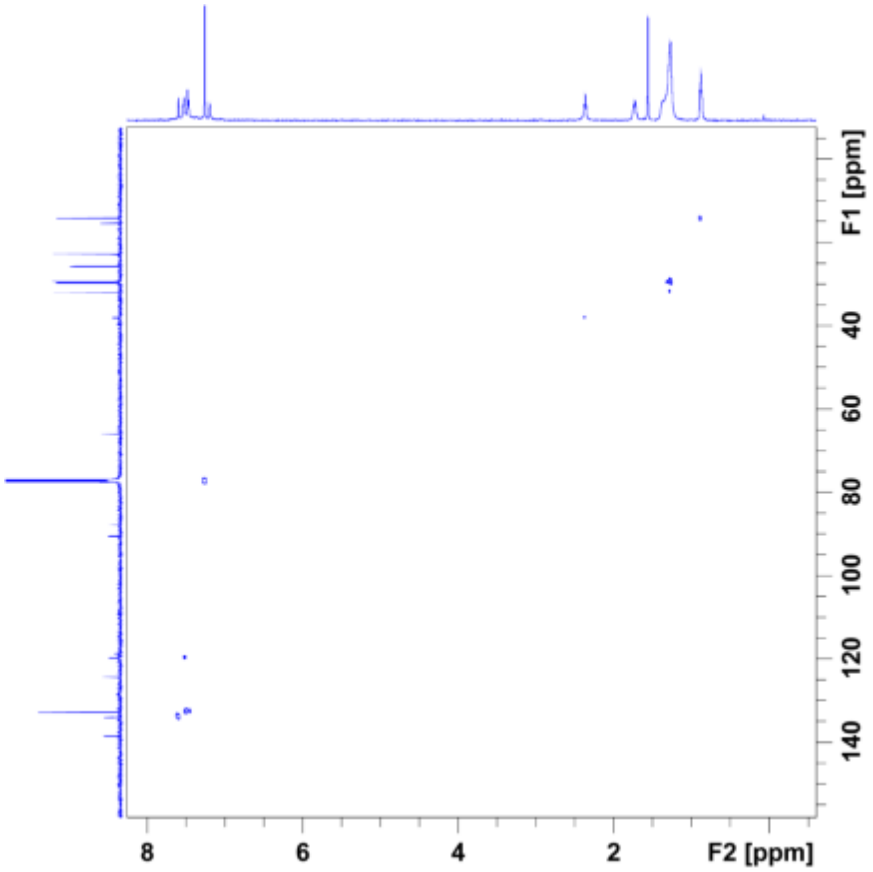

^{1}H, ^{13}C-HMQC spectrum ($CDCl_3$, 298 K) of compound **1a**.

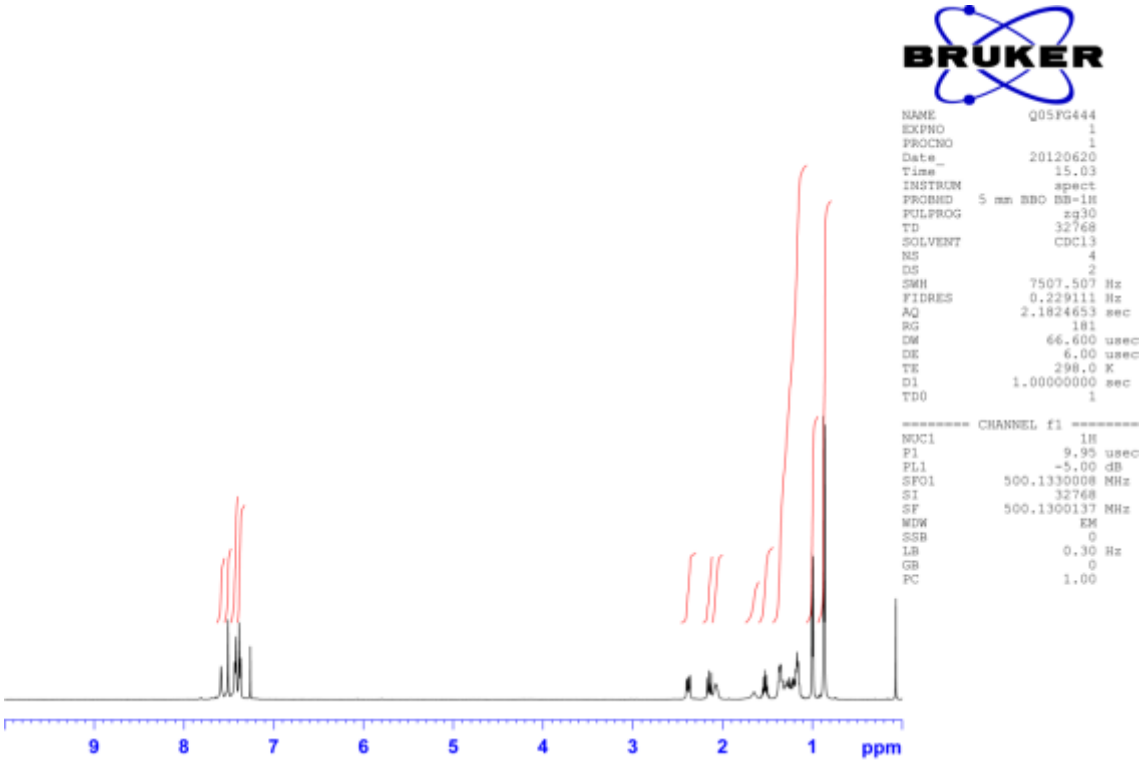

^{1}H NMR ($CDCl_3$, 500 MHz, 298 K) of compound **1b.**

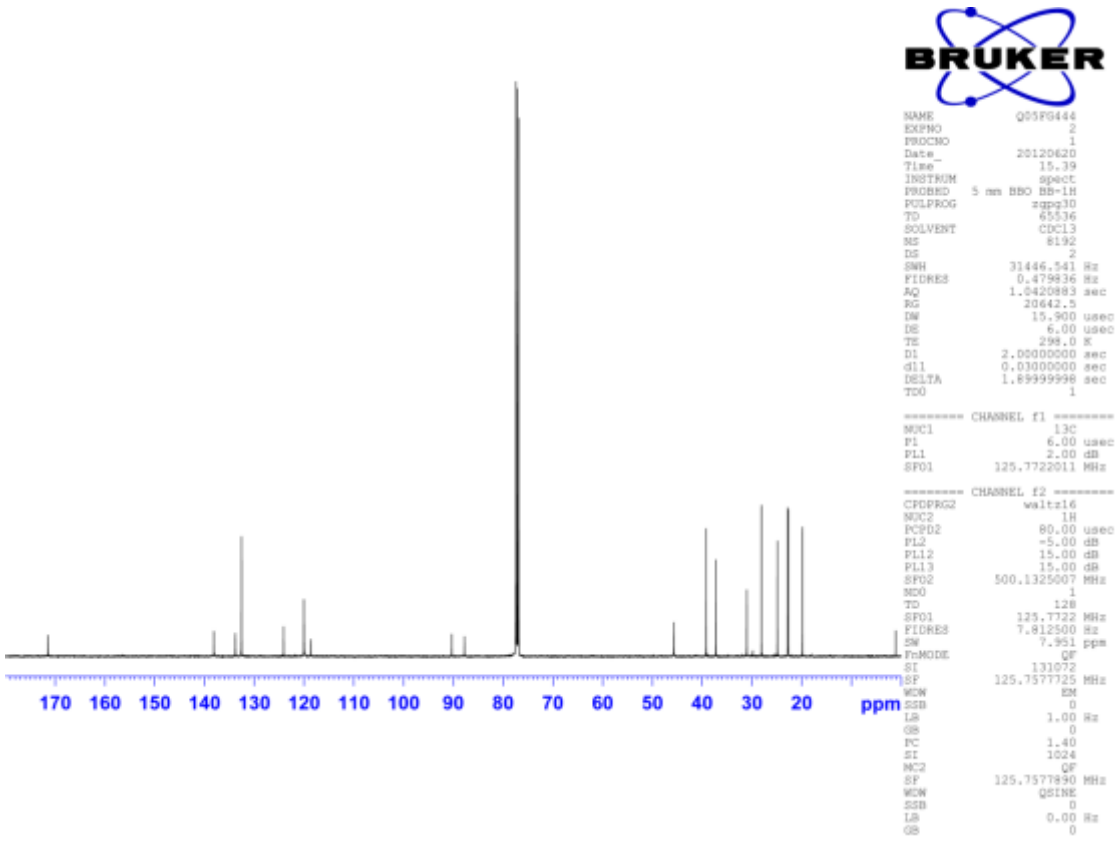

^{13}C NMR ($CDCl_3$, 125 MHz, 298 K) of compound **1b**.

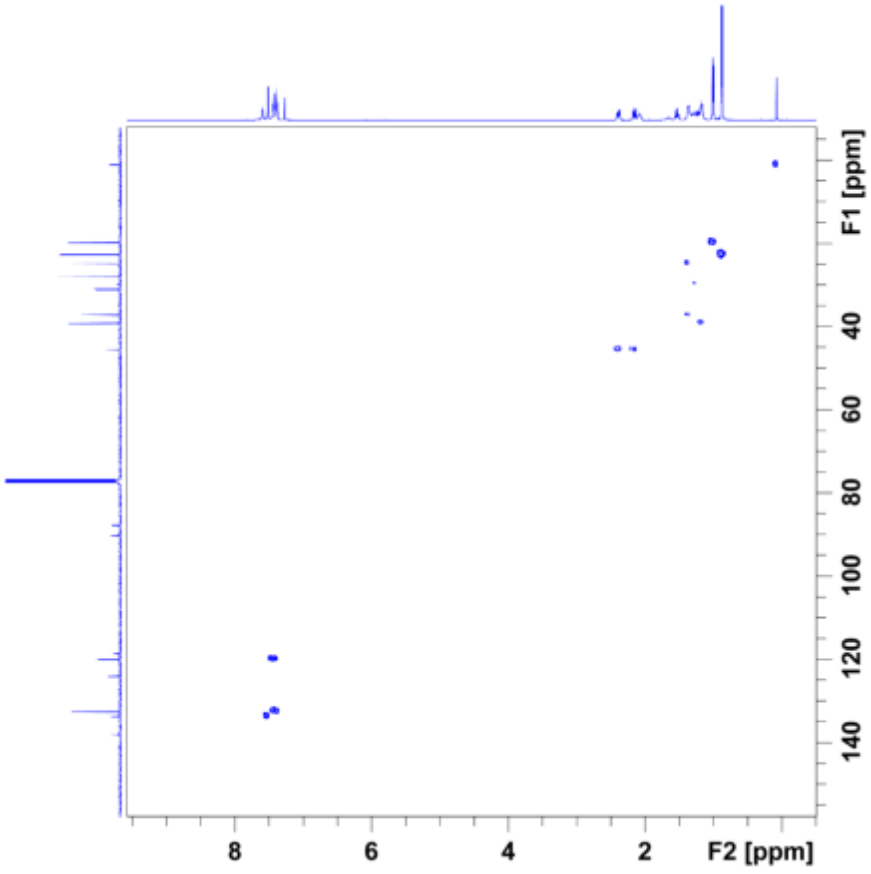

^{1}H, ^{13}C-HMQC spectrum ($CDCl_3$, 298 K) of compound **1b**.

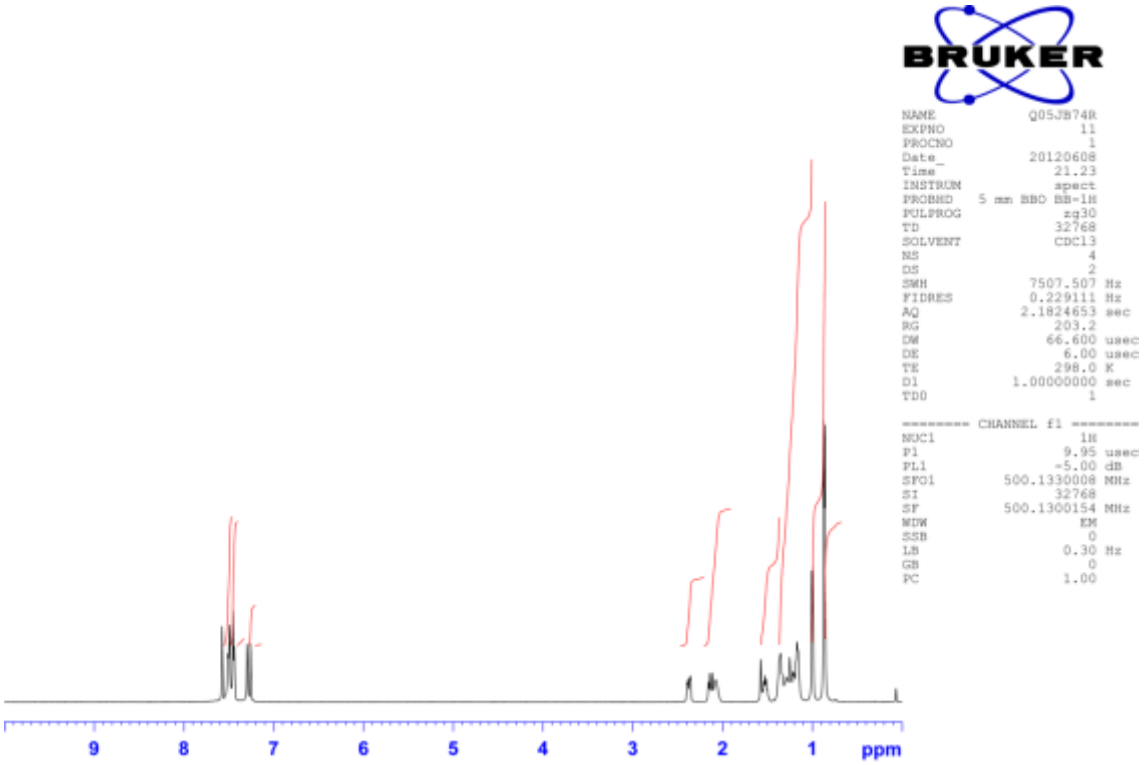

^{1}H NMR ($CDCl_3$, 500 MHz, 298 K) of compound **1c**.

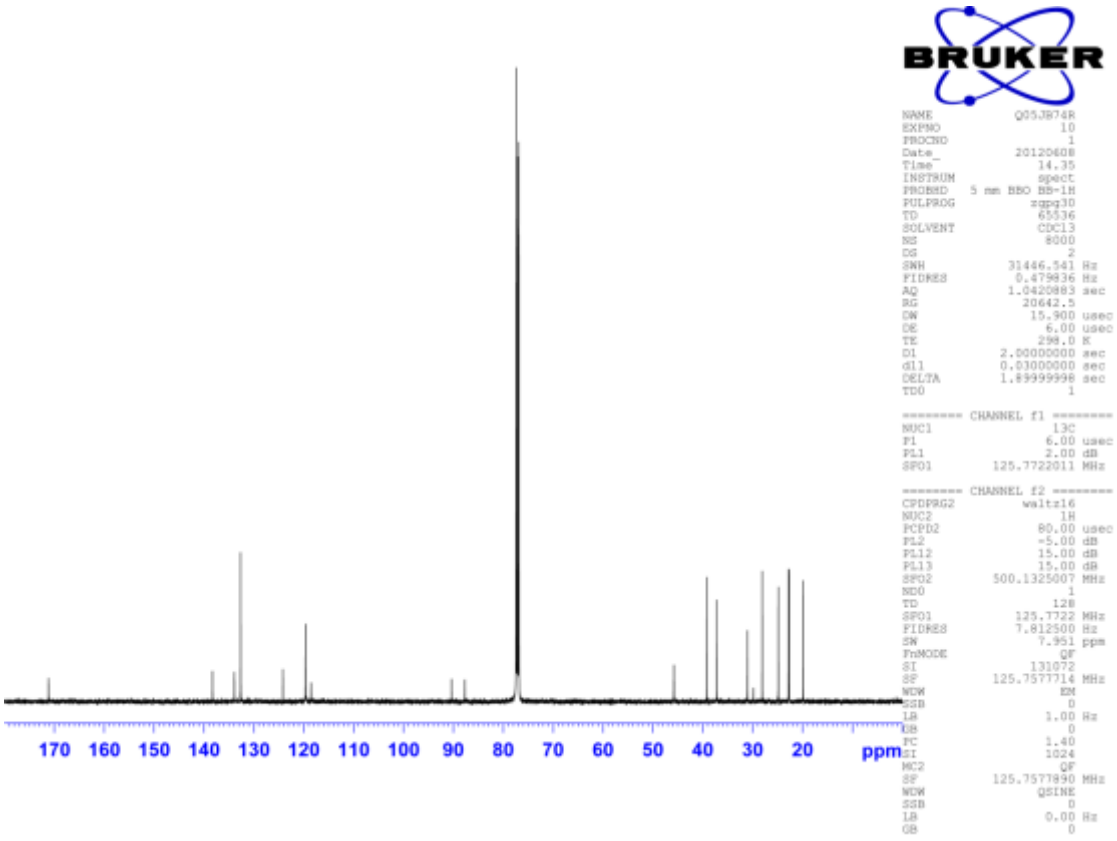

^{13}C NMR ($CDCl_3$, 125 MHz, 298 K) of compound **1c**.

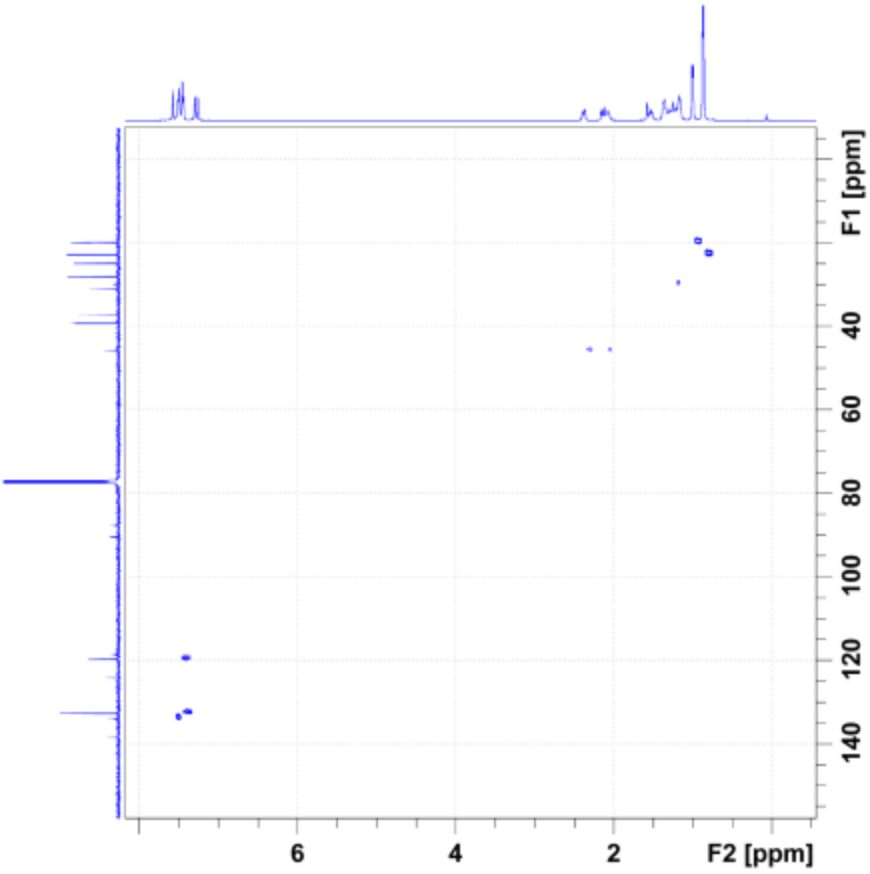

^{1}H, ^{13}C-HMQC spectrum ($CDCl_3$, 298 K) of compound **1c**.